A New Poisson Noisy Image Denoising Method Based on the Anscombe Transformation

Jin Quan[1], William G. Wee[1], Chia Y. Han[2], and Xuefu Zhou[1]
[1]School of Electronic and Computing Systems, University of Cincinnati, Cincinnati, OH, 45221, USA
[2]School of Computing Sciences and Infomatics, University of Cincinnati, Cincinnati, OH, 45221, USA

Abstract— *In this paper, we propose a new denoising method for Poisson noise corrupted images based on the Anscombe variance stabilizing transformation (VST) with a new inversion. The VST is used to approximately convert a Poisson noise image into a Gaussian distributed image, so that the denoising methods aiming at Gaussian noise can be applied subsequently. The motivation for the new inversion originates from a main drawback existing in the Anscombe transformation: its efficiency degrades significantly when the pixel intensities of the observed images are very low due to the biased errors generated by its inverse transformation. Thus, we introduce a polynomial regression model in the sense of weighted least squares as an improvement for the inverse Anscombe transformation. Moreover, we incorporate our developed wavelet thresholding strategy for Gaussian noise into the proposed method. It is shown in the experimental analysis that this method is very competitive for Poisson denoising.*

Keywords: Poisson noise, image denoising, Anscombe transformation, wavelet transform

1. Introduction

The intensity of a certain pixel in an observed image is approximately proportional to the photon counts arrived in it. These photons are obtained by a detection device like CCD. Normally, noise will invariably be introduced by the errors in the detection device itself due to its lack of infinite precision. In addition, noise can also arise when photons travel from the object to the detection device. Thus, it is necessary to employ image restoration approaches so that the noise on the obtained image can be suppressed such that people can be provided with an improved observation of the object of interest.

Low-intensity images, where relatively few photons are observed or the counts of photons arrived on the detection device are very limited, are common in many of the image processing applications in the biomedical and astronomic domains. In these situations, many well-established existing image restoration methods designed for handling additive white Gaussian noise (AWGN) become expectably unfitted because the models are usually only appropriate when the number of photon counts per pixel is relatively large. But a reasonable assumption to make for low intensity images due to limited photon counts is that the observed image can be considered as a realization of a Poisson process and the photon counts of pixels can be modeled as Poisson distribution. Thus, a photon-limited image can be modeled as a 2D matrix of Poisson variables. The modeling of Poisson process is very different from that of the Gaussian process. In Gaussian models, the variance of the noise is stationary, whereas the variance of Poisson noise is non-stationary throughout the whole image and the magnitude of the noise is dependent on the pixel intensity that we want to restore which makes removing noise of this type a more difficult problem.

Fortunately, there exists a simple and intuitive, widely used procedure for Poisson denoising in practice. The core principle of this procedure is to transform the Poisson variables into Gaussian variables thus the existing denoising algorithms treating the AWGN can be applied. It has three main steps: 1) a variance stabilizing transformation (VST) is executed on the obtained Poisson noisy image so that the noise variance is approximately stabilized through the whole image; 2) an existing AWGN denoising algorithm such as state-of-the-art approaches [1], [2] is then applied on this transformed image; 3) an inverse transformation is used on this transformed and processed image resulting in the final recovered image. This Poisson noisy image denoising procedure is illustrated in Figure 1.

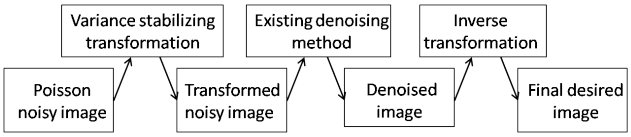

Fig. 1: General Poisson noisy image denoising procedure

Other than the classical VST solution mentioned above, major contributions are made under different frameworks. Kolaczyk [3] has developed soft and hard thresholds for Poisson intensities as an adapted version of the usual Gaussian-based universal thresholds designed for AWGN [4]. In [5], Mäkitalo and Foi introduce new inversions including a maximum likelihood inversion and a minimum mean square error inversion for the commonly used VST: Anscombe transformation [6]. They combine these inversions with BM3D technique, which is a state-of-the-art

denoiser for AWGN and consistently improved performances are achieved. In [7], Zhang *et al*. present a modified VST to efficiently stabilize the Poisson distributed data while incorporating some multi-resolution transforms such as ridgelets and curvelets. Their algorithm especially aims at very low-intensity signals. In [8], Luisier *et al*. propose a Poisson denoising algorithm PURE-LET based on an unnormalized Haar wavelet transform and the minimization of an unbiased estimate of the MSE for Poisson noise. Their method is very competitive in terms of denoising performance and computational complexity. Willett and Nowak [9] employ a Poisson intensity estimation approach involving a platelet-based penalized likelihood estimation of a piecewise polynomial on recursive dyadic partitions of the support of the Poisson intensity. Its estimator does not require any *a priori* knowledge of the clean signal's smoothness.

In this paper, we propose a new Poisson denoising approach adopting the aforementioned traditional VST solution, but with a more precise inverse transformation model. The proposed inverse Anscombe transformation (IAT) corrects the biased errors brought by the conventional inverse Anscombe transformations in the sense of weighted least squares. This whole approach guarantees a success of the denoising process by incorporating our new competitive denoising method [10] based on context modeling (CM) and wavelet thresholding (WT) and is designed for AWGN, hereafter termed *CMWT-IAT*. The performance of CMWT-IAT method shown from the quantitative results reveals that it is indeed a promising competitor for Poisson denoising. Other main advantages of our approach include that it is simple and easy to implement, requires minimum human interaction and relatively low computational burden.

The rest of this paper is organized as follows. In Section 2, we briefly recall the Poisson distributed model and the Anscombe transformation as well as its conventional inverse transformations. In Section 3, we propose the CMWT-IAT method with a new piecewise polynomial regression model for inverse transformation. In Section 4, various experiments are included to verify the efficiency of the CMWT-IAT method. Finally, the conclusion is presented in Section 5.

2. Poisson Model and Anscombe Transformation

Suppose $y = (y_i)_{i\in\Re^2}$ is an image we obtained and each pixel intensity y_i can be modeled as a Poisson random variable following this probability density function

$$P_{x_i}(y_i) = \frac{e^{-x_i}{x_i}^{y_i}}{y_i!}, y_i \geq 0 \tag{1}$$

where the Poisson parameter x_i is not only the mean value of y_i, but also equals to its variance σ_i^2.

We assume that the mean value x_i of each observed pixel intensity y_i is its corresponding pixel intensity in the clean image and the variability of the mean can be interpreted as noise. Therefore, our goal is to restore the original clean image $x = (x_i)_{i\in\Re^2}$ by searching for an estimate $\hat{x} = (\hat{x}_i)_{i\in\Re^2}$ which is as close as possible to x given that observed noisy image y.

Usually, the closeness between the estimate and original image is measured in terms of minimum mean square error

$$\mathrm{MSE} = \frac{1}{N}||\hat{x} - x||^2 = \frac{1}{N}\sum_{i=1}^{N}(\hat{x}_i - x_i)^2 \tag{2}$$

where N is the total number of pixels in the image.

The denoising problem can also be stated as to estimate the underlying mean value $x = (x_i)_{i\in\Re^2}$ of each pixel from a realization of the Poisson process.

The main obstacle for many existing Gaussian denoising algorithms to be directly applied on noisy photon-limited images is that they are unable to model the variance of the Poisson noise as non-stationary and dependent on the underlying intensity. Thus, several VST methods such as those in [7], [11] are used to remove the dependence of the noise variance on the underlying data. Among them, we choose the classic Anscombe transformation [6] since it is still widely used and considered to be a useful tool due to its efficiency and simplicity. Its expression is as follows

$$Y_i = \mathrm{T}(y_i) = 2\sqrt{y_i + \frac{3}{8}} \tag{3}$$

where y_i is the observed intensity value of Poisson noisy image and Y_i is the transformed intensity value. From now on, we use uppercase letters to represent the corresponding transformed data.

After the Anscombe transformation T, the pixel intensities throughout the whole image are approximately Gaussian distributed with mean 0 and variance $\sigma^2 = 1$. Thus its variance is assumed to be stationary.

We suppose that there is a promising denoising operation available which provides a successful transformed estimate $\hat{X}$ based on the observed y. In practice, after the denoising operation is performed, it is necessary to apply an inverse transformation in order to obtain the final estimate $\hat{x}$ of the original data. So the arithmetical inverse Anscombe transformation f_1 is naturally derived as

$$\hat{x}_i = f_1(\hat{X}_i) = \mathrm{T}^{-1}(\hat{X}_i) = \left(\frac{\hat{X}_i}{2}\right)^2 - \frac{3}{8} \tag{4}$$

Though very simple, it is emphasized in [5] that this inverse transformation fails to be competent when being applied to those variables with low values since the resulting estimate $\hat{x}$ inevitably generates biased errors due to the nonlinearity of the forward Anscombe transformation T, so that we have

$$E\{\mathrm{T}(y)|x\} \neq \mathrm{T}(E\{y|x\}) \tag{5}$$

and thus

$$\mathrm{T}^{-1}(E\{\mathrm{T}(y)|x\}) \neq (E\{y|x\}) \tag{6}$$

Meanwhile, it is worth noting that we can also choose an alternative to the arithmetical inverse Anscombe transformation, which relatively mitigates the biased error for smaller valued Poisson parameters. It is called asymptotical inverse Anscombe transformation f_2 and its expression is as [6]

$$\hat{x}_i = f_2(\hat{X}_i) = \left(\frac{\hat{X}_i}{2}\right)^2 - \frac{1}{8} \tag{7}$$

Nevertheless, the main drawback of this inverse transformation is similar to that of the arithmetical inverse transformation, that is its performance on very low values falls out of satisfaction. Thus, in order to minimize the bias error in low-intensity images, in the next section we propose a more precise inverse transformation.

3. The CMWT-IAT Method to Poisson Denoising

As previously mentioned, generally the efficiency of either the arithmetical or asymptotical inverse Anscombe transformation only holds under the assumption that the underlying mean value is large enough, but their reliability is invalid for those Poisson variables with relatively small mean values and their performances deteriorate quickly. Hence basically we are interested to get a quantitative idea of how large the biased errors become when the underlying Poisson variables are small enough after the forward transformation.

Accordingly, for each integer i from 1 to 255, we generate a data set consisting of a very large number of Poisson variables with i being the underlying Poisson parameter. We then calculate the variance of this data set for each i. The results are shown in Figure 2a, from which we observe that it follows the Poisson property that the variance is approximately equal to the mean value. Then, we apply the Anscombe transformation (3) on all the variables in these data sets, calculate the variance of each transformed data set, and illustrate the results in Figure 2b. The figure reveals that the variances are almost equal to 1 with little respect to the mean value i throughout the entire range of the corresponding underlying Poisson parameters, with only negligible oscillation.

We then explore the biased errors between the transformed parameters and their estimated means and show them in Figure 3. The x axis denotes the Poisson parameters, and y axis denotes the mean values estimated from the Anscombe transformed Poisson data for each parameter i, but with each value divided by the mean value of the original Poisson variables. By observing the figure, it is clearly seen that both values are almost identical to each other from a practical standpoint of view when the value of a Poisson parameter is

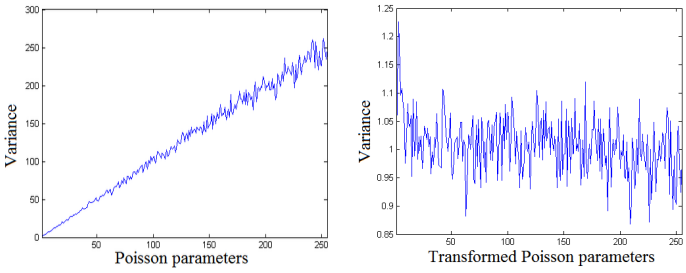

(a) (b)

Fig. 2: (a) Variance of Poisson distributed data sets, (b) Variance of the transformed data sets

no less than 30. Thus, it is reasonable to consider that after applying Anscombe transformation, the Poisson variables are unbiased as long as the values are no less than 30. It indicates that both the arithmetical and asymptotical inverse Anscombe transformations still work effectively in such a situation so that we can apply either of them directly.

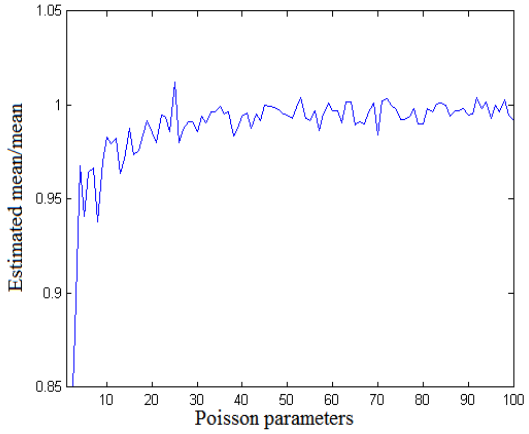

Fig. 3: Biased errors between Poisson parameters and estimated means

But for Poisson parameters with values less than 30, the resulting values are severely underestimated especially when they are below 10. Consequently, our main focus at this stage is to develop a solution appropriately applicable to the inversion of Poisson parameters with relatively small values. Thus, it is intuitive for us to compensate the denoised results before the arithmetical inversion by adaptively dividing a predefined factor for each obtained Poisson estimate. This factor can be derived by fitting the curve in Figure 3 in a least squares sense using the linear polynomial regression model

$$b_i = \mathrm{P}(a) = p_1 a_i^n + p_2 a_i^{n-1} + ... + p_n a_i + p_{n+1} \tag{8}$$

where $n+1$ is called the order of the polynomial and n is called the degree of this polynomial.

In order to calculate the estimated coefficients in the polynomial, the minimization of the following summation of the weighted squares is required.

$$\text{minimize} \quad S = \sum_{i=1}^{K} w_i r_i^2 = \sum_{i=1}^{K} w_i (b_i - \hat{b}_i)^2 \tag{9}$$

where r_i, the residual, is defined as the difference between the measured value b_i and the fitted value $\hat{b}_i$; K is the number of data points provided in the fit; w_i is the weight which determines how much each corresponding value influences the final estimate. For simplicity, we set the weights as

$$w_i = \frac{1}{\sigma_i^2} \tag{10}$$

where each σ_i^2 is derived from the variance of the transformed Poisson data from Figure 2b.

When fitting the curve by polynomials, we also assume that there exist random variations in the measured data and the random variations are Gaussian distributed with a zero mean and variance σ^2. We add this error in the polynomial expressed as

$$b_i = \mathrm{P}(a) = p_1 a_i^n + p_2 a_i^{n-1} + ... + p_n a_i + p_{n+1} + \varepsilon_i \tag{11}$$

where $\varepsilon_i \sim N(0, \sigma^2), \ \forall i$ and $\mathrm{cov}(\varepsilon_i, \varepsilon_j) = 0, \ \forall i, j$
In matrix notation, the polynomial regression model is given by

$$\mathbf{b} = \mathbf{A}\mathbf{p} + \boldsymbol{\varepsilon} \tag{12}$$

The solution vector $\mathbf{p}$ can be obtained by solving

$$\mathbf{p} = (\mathbf{A}^\mathbf{T}\mathbf{W}\mathbf{A})^{-1}\mathbf{A}^\mathbf{T}\mathbf{W}\mathbf{b} \tag{13}$$

where $\mathbf{W}$ consists of the diagonal elements of the weight matrix $\mathbf{w}$.

With the polynomial regression model, the flexibility for the data is desirably achieved. However, if the degree of the polynomial is high, the fitting model becomes dramatically unstable. We should also note that the polynomial regression model is expected to work only within a certain range, and divergence can be caused significantly out of this range. Thus the suitable range has to be selected carefully. For this consideration, we suggest the polynomials for our application be piecewise and quadratic or cubic.

We hereby separate the curve in Figure 3 into three segments before using the polynomial regression model to fit: 1) Poisson parameters with values under 10, 2) those with values from 10 to 30 and 3) those with values larger than 30. For the first two groups, illustrated in Figure 4a and 4b, with the coefficient vector $\mathbf{p}$ known from (13) for the fitting polynomial and denoised transformed estimate $\hat{X}_i$, the final desired value of $\hat{x}_i$ can be obtained by

$$\hat{\hat{X}}_i = \frac{\hat{X}_i}{\sum_{j=1}^{m} p_j \hat{X}_i^{m-j} + \varepsilon_i} \tag{14}$$

$$\hat{x}_i = \left(\frac{\hat{\hat{X}}_i}{2}\right)^2 - \frac{3}{8} \tag{15}$$

where m is the order of the polynomial, $\hat{\hat{X}}_i$ is the corrected denoised estimate in the transformed domain.

Furthermore, if the value of a Poisson variable is larger than 30, the asymptotical inverse Anscombe transformation (7) is adopted.

So far, we have provided detailed explanations for the first and third steps in the Poisson denoising procedure stated in Section 1. For the second step–the denoising part, we apply our developed wavelet based denoising method for AWGN [10], which yields very competitive performances. For the readers' convenience, its brief procedure is summarized here:

1) Perform multilevel discrete wavelet transform (DWT) on the input noisy image y to produce its wavelet representation Y.
2) Estimate a smoothed version Z from Y using $Z_i = w^t u_i$ where the weight w is calculated in terms of minimizing mean squared error, and u_i is a vector consisting of Y_i's relevant coefficients.
3) Estimate the additive white Gaussian noise standard deviation of noisy image y.
4) Add portion of noisy Y to Z to form a newer version Z' adaptively for different subbands and noise levels.
5) Determine the parameters of the optimized soft thresholding operation on Z' and compute the estimate $\hat{X}$ by adding offsets adaptively to a close formed solution.
6) Apply inverse DWT on $\hat{X}$ to obtain the denoised image $\hat{x}$.

Furthermore, in order to suppress the unpleasant Pseudo-Gibbs phenomena in the area such as edges and ridge discontinuities in images after standard wavelet denoising, we carry out an overcomplete expansion process called *cycle spinning* originally proposed in [12]. The basic procedure of it is to circularly shift the input image to generate a set of images as its overcomplete representations,

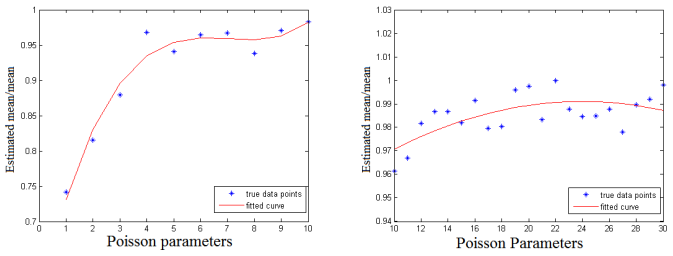

Fig. 4: (a) Curve fitting for Poisson parameter under 10, (b) Curve fitting for Poisson parameter from 10 to 30

then do the same denoising operation on each of them, and shift back before averaging all the denoised representations to obtain the final desired image. By applying this strategy, we can remove some disturbing visual artifacts so that the denoised image's quality is notably improved.

4. Experiments

The proposed denoising method CMWT-IAT on Poisson noise corrupted images shows theoretical reliability and we conduct three groups of experiments to confirm its actual performance. In our experiments, we take the commonly favored peak signal-to-noise ratio (PSNR) as our measurement of the denoising performance, which is defined as

$$\mathrm{PSNR} = 10\log_{10}(\frac{I_{\max}^2}{\mathrm{MSE}}) \tag{16}$$

where MSE is defined in (2) and $I_{\max}$ is the largest intensity of the noise-free image.

Since Poisson modeled denoising methods are specifically applicable on the photon-limited images, it is more reasonable to conduct our empirical experiments in a low-intensity setting. For this reason, the intensities of pixels on six standard testing images are scaled down proportionally with the maximum intensity $I_{\max}$ being 60, 30, 20, 10 and 5 respectively and Poisson noise is added to each of them.

A.Experiment 1

In this experiment, we verify the advantage of our proposed inverse transformation over both the arithmetical and asymptotical inverse Anscombe transformations in (4,7). In all three methods, we denoise the transformed images using our method presented in [10] with the overcomplete representation. The only difference is the inverse transformations used after the denoising.

In Table 1, we present the PSNR comparisons between these three different transformations. From the table, we can notice that our proposed inverse method apparently yields significant improvements than the other two when the peak intensity is low.

B.Experiment 2

We illustrate the efficiency of our developed denoising method [10] when being applied on the transformed Poisson data in this experiment. We compare it with a state-of-the-art Gaussian denoising algorithm SURE-LET [13] under non-overcomplete wavelet transform. For both methods, we apply our proposed inverse transformation. Here the PSNR values of our method are also obtained by using non-overcomplete wavelet transform. These numerical results are presented in Table 2.

In Figure 5, we show visual results of both denoising methods applied on Image *Man*. We can notice that the delicate details such as the man's hair and feathers on the image obtained by CMWT-IAT are less over-smoothed and better restored.

From the numerical results and visual comparison, it is convinced that our denoising method originally designed for AWGN is still a very viable and effective approach when applying on the variance stabilized Poisson data and it generates significantly superior results than SURE-LET in a low-intensity setting.

C.Experiment 3

In this group of experiments, we compare the following denoising methods on their performances of denoising low-intensity images and list the PSNR results in Table 3 for different images and peak intensities.

• SURE-LET

A combination of an overcomplete wavelet transform denoising approach [14] derived from their state-of-the-art method [13] and our proposed inverse transformation applied after the denoising. It consists of a denoising estimator derived from a series of weighted and optimized thresholding functions.

• PURE-LET

A competitive Poisson intensity restoration technique [7]. It minimizes an unbiased estimate of the MSE for Poisson noise and the denoising process is a linear combination of optimized thresholding functions. The denoising results of this approach are obtained by applying 10 cycle spins in our simulations.

• BM3D

Table 1: PSNR (dB) comparison of the arithmetical, asymptotical inverse Anscombe transformations and the proposed inverse transformation

Image	Peak	Arithmetical	Asymptotical	Proposed
Lena	5	23.11	25.30	**25.98**
	10	25.91	27.20	**27.23**
	20	28.43	28.98	**28.99**
	30	29.68	**29.95**	**29.95**
	60	31.32	31.45	**31.46**
Goldhill	5	23.27	25.72	**26.11**
	10	25.85	26.88	**26.92**
	20	27.77	**28.29**	**28.29**
	30	28.61	**28.86**	**28.86**
	60	30.16	**30.26**	**30.26**
Boat	5	22.76	24.80	**25.18**
	10	25.45	26.53	**26.64**
	20	27.69	27.72	**27.73**
	30	28.26	28.48	**28.50**
	60	30.05	**30.15**	**30.15**
Barbara	5	21.68	23.26	**23.55**
	10	23.81	24.51	**24.61**
	20	25.62	25.96	**25.97**
	30	26.66	**28.85**	**28.85**
	60	29.04	29.12	**29.13**
Couple	5	22.60	24.81	**25.10**
	10	25.15	26.07	**26.28**
	20	27.18	27.61	**27.63**
	30	28.13	28.39	**28.40**
	60	29.91	30.01	**30.03**
Man	5	22.96	25.16	**25.53**
	10	25.71	26.83	**26.89**
	20	27.37	**27.84**	**27.84**
	30	28.31	**28.54**	**28.54**
	60	29.95	**30.04**	**30.04**

A combination of non-wavelet denoising method BM3D and their inverse transformation [5]. BM3D is a state-of-the-art denoising algorithm using sparse 3D transform domain collaborative filtering [2]. In addition, their unbiased inverse transformation is based on minimum likelihood (ML) and minimum mean square error (MMSE).

• CMWT-IAT

A combination of applying the overcomplete representation of our wavelet based denoising method [10] for AWGN and the proposed inverse transformation presented in this paper.

From Table 3, in general, CMWT-IAT's performance is very competitive in terms of PSNR. In particular, it outperforms SURE-LET and PURE-LET with an improvement up to 1.5 dB. Meanwhile, it is interesting to mention that by using the proposed inverse transformation, SURE-LET essentially produces better results than the specified Poisson denoiser PURE-LET. Besides, CMWT-IAT can yield comparable or even improved results to the state-of-the-art BM3D approach, especially for the Images *Goldhill* and *Man*. We found out that for the Images *Lena* and *Barbara*, our algorithm is not able to yield a similar performance to BM3D. We analyze that it is due to the limitation of our wavelet modeling in estimating the dominated recurrent textures such as Lena's hat and Barbara's pants in these images.

We also provide a set of Image *Goldhill* obtained by different denoising methods for visual comparison in Figure 6. We can point out that the proposed denoising method CMWT-IAT which combines our wavelet based denoising method and the proposed inverse transformation yields very few disturbing artifacts and keeps more useful features like the grids on the windows compared to the other methods.

Table 2: PSNR (dB) comparison of SURE-LET [13] and CMWT-IAT for different images and peak intensities

Image	Peak	Noisy	SURE-LET	CMWT-IAT
Lena	5	9.93	24.42	**25.31**
	10	12.95	**26.73**	26.56
	20	15.98	28.21	**28.42**
	30	17.72	29.07	**29.38**
	60	20.74	30.69	**30.87**
Goldhill	5	10.22	23.16	**25.52**
	10	13.23	25.23	**26.41**
	20	16.24	26.52	**27.86**
	30	17.99	27.29	**28.47**
	60	20.99	28.66	**29.80**
Boat	5	9.93	22.82	**24.60**
	10	12.94	25.02	**25.80**
	20	15.96	26.53	**27.25**
	30	17.73	27.33	**28.03**
	60	20.70	28.88	**29.55**
Barbara	5	10.20	21.23	**23.15**
	10	13.21	23.10	**24.21**
	20	16.24	24.38	**25.56**
	30	17.98	25.36	**26.47**
	60	20.99	27.08	**28.56**
Couple	5	10.20	22.72	**24.55**
	10	13.23	24.75	**25.75**
	20	16.24	26.15	**27.18**
	30	17.99	27.03	**27.96**
	60	21.03	28.55	**29.48**
Man	5	10.32	22.80	**24.95**
	10	13.33	25.08	**26.01**
	20	16.36	26.41	**27.39**
	30	18.14	27.24	**28.14**
	60	20.11	28.74	**29.59**

5. Conclusion

In this paper, we have presented a new denoising method called CMWT-IAT for Poisson noise corrupted images. The method uses the Anscombe variance stabilizing transformation and combines our previously developed wavelet-based Gaussian denoising method with a new proposed inverse transformation based on a polynomial regression model. By applying this method, the biased errors produced by conventional inversions have been significantly corrected. Though simple and easy to implement, it is considered to be very effective on photon-limited images. In empirical experiments, we have shown that it outperforms two widely used Anscombe inverse transformations as well as some leading image restoration methods. The quantitative and

Fig. 5: (a) Part of the original Image *Man* at peak intensity 30. (b) Poisson noise corrupted image. (c) Image denoised with non-overcomplete SURE-LET [13] and the proposed inversion. (d) Image denoised with the proposed method CMWT-IAT.

Table 3: PSNR (dB) comparison of some of the best denoising methods for different images and peak intensities

Image	Peak	SURE-LET	PURE-LET	BM3D	CMWT-IAT
Lena	5	25.84	24.74	**26.56**	25.98
	10	27.55	26.68	**28.31**	27.23
	20	29.08	27.81	**29.99**	28.99
	30	29.97	29.16	**30.96**	29.95
	60	31.42	30.94	**32.43**	31.46
Goldhill	5	24.54	23.48	24.92	**26.11**
	10	26.04	25.59	26.33	**26.92**
	20	27.25	26.38	27.75	**28.29**
	30	28.04	27.42	28.55	**28.86**
	60	29.36	28.92	29.92	**30.26**
Boat	5	24.07	23.68	24.77	**25.18**
	10	25.75	25.33	26.28	**26.64**
	20	27.22	26.41	**27.83**	27.73
	30	28.05	27.51	**28.74**	28.50
	60	29.64	29.15	**30.29**	30.15
Barbara	5	22.16	22.61	**24.48**	23.55
	10	23.50	23.56	**26.35**	24.61
	20	24.76	24.80	**28.18**	25.97
	30	28.05	27.51	**29.19**	28.50
	60	27.52	27.52	**30.91**	29.13
Couple	5	23.99	23.35	24.46	**25.10**
	10	25.53	25.01	26.14	**26.28**
	20	27.05	26.24	**27.74**	27.63
	30	27.97	27.19	**28.77**	28.40
	60	29.53	28.94	**30.37**	30.03
Man	5	24.06	23.65	24.77	**25.53**
	10	25.71	25.57	26.13	**26.89**
	20	27.00	26.13	27.54	**27.84**
	30	27.83	27.32	28.35	**28.54**
	60	29.30	28.91	29.83	**30.04**

visual results both verify that it is very competitive with the existing methods in denoising Poisson noise corrupted images.

Fig. 6: (a) Part of the original Image *Goldhill* at peak intensity 20. (b) Poisson noise corrupted image. (c) Image denoised with overcomplete SURE-LET [14] and the proposed inversion. (d) Image denoised with PURE-LET [8]. (e) Image denoised with BM3D and their unbiased inversion [5]. (f) Image denoised with the proposed method CMWT-IAT.

References

[1] J. Portilla, V. Strela, M. J. Wainwright, and E. P. Simoncelli, "Image denoising using scale mixtures of Gaussians in the wavelet domain," *IEEE Trans. Image Process.*, vol. 12, no. 11, pp. 1338-1351, Nov. 2003.

[2] K. Dabov, A. Foi, V. Katkovnik, and K. Egiazarian, "Image denoising by sparse 3D transform-domain collaborative filtering," *IEEE Trans. Image Process.*, vol.16, no.8, pp. 2080-2095, Aug. 2007.

[3] E. D. Kolaczyk, "Wavelet shrinkage estimation of certain Poisson intensity signals using corrected thresholds," *Statist. Sinica*, vol. 9, pp. 119-135, 1999.

[4] D. L. Donoho and I. M. Johnstone, "Ideal spatial adaptation via wavelet shrinkage," *Biometrika*, vol. 81, pp. 425-455, 1994.

[5] M. Mäkitalo and A. Foi, "Optimal inversion of the Anscombe transformation in low-count Poisson image denoising," *IEEE Trans. Image Process.*, vol. 20, no. 1, pp.99-109, Jan. 2011.

[6] F. J. Anscombe, "The transformation of Poisson, binomial and negative binomial data," *Biometrika*, vol. 35, no. 3/4, pp.246-254, 1948.

[7] B. Zhang, J. M. Fadili, and J.-L. Starck, "Wavelets, ridgelets, and curvelets for Poisson noise removal," *IEEE Trans. Image Process.*, vol. 17, no. 7, pp. 1093-1108, Jul. 2008.

[8] F. Luisier, C. Vonesch, T. Blu, and M. Unser, "Fast interscale wavelet denoising of Poisson-corrupted images," *Signal Process.*, vol. 90, no.2, pp. 415-427, Feb. 2010.

[9] R. M. Willett and R. D. Nowak, "Multiscale Poisson intensity and density estimation," *IEEE Trans. Inf. Theory*, vol. 53, no. 9, pp. 3171-3187, Sep. 2007.

[10] J. Quan, W. G. Wee, and C. Y. Han, "A new wavelet based image denoising method," *IEEE Data Compression Conference (DCC'12)*, pp. 408, Snowbird, UT, Apr. 2012.

[11] P. Fryzlewicz, G.P. Nason, "A Haar-Fisz algorithm for Poisson intensity estimation," *Journal of Computational and Graphical Statistics*, vol. 13 no. 3, pp. 621-638, 2004.

[12] R. R. Coifman and D.L. Donoho, "Translation-invariant de-noising," *Wavelets and Statistics*, A. Antoniadis and G. Oppenheim eds., Sprigner-Verlag Lecture Notes, pp.125-150, 1995.

[13] F. Luisier and T. Blu, "A new SURE approach to image denoising: interscale orthonormal wavelet thresholding," *IEEE Trans. Image Process.*, vol. 16, No. 3, pp. 593-606, Mar. 2007.

[14] T. Blu and F. Luisier, "The SURE-LET approach to image denoising," *IEEE Trans. Image Process.*, vol. 16, no. 11, pp. 2778-2786, Nov. 2007.